Journal of the Optical Society of Korea
Vol. 17, No. 6, December 2013, pp. 471-480
DOI: http://dx.doi.org/10.3807/JOSK.2013.17.6.471

Enhancing the Performance of Coherent Sources SAC OCDMA Networks via Spatial Multiplexing

Ahmed M. Alhassan[1]*, Nasreen Badruddin[1], Naufal M. Saad[1], and Syed A. Aljunid[2]

[1]Depatrment of Electrical and Electronics Engineering, Universiti Teknologi PETRONAS (UTP), Tronoh, Perak, Malaysia
[2]School of Computer and Communication Engineering, Universiti Malaysia Perlis (UniMAP), Arau, Perlis, Malaysia

(Received August 19, 2013 : revised October 22, 2013 : accepted October 22, 2013)

The beating of two or more lasers that have the same or a finite difference in the central frequencies, is the main source of noise in spectral amplitude coding optical code division multiple access (SAC OCDMA) systems. In this paper we adopt a spatial multiplexing (SM) scheme for SAC OCDMA systems to mitigate this beat noise. The results show that for different code weights and different data rates SM SAC can support a larger number of users than the conventional SAC for all different laser source configurations. However, SM SAC requires a more complex system than the conventional SAC, and almost twice as much optical component.

Keywords : Optical code division multiple access (OCDMA), Spectral amplitude coding (SAC) OCDMA, Spatial multiplexing, Coherent sources
OCIS codes : (060.2330) Fiber optics communications; (060.4230) Multiplexing

I. INTRODUCTION

All future access networks will deploy fiber optics technology to provide end users with the required bandwidth to feed all bandwidth-hungry applications. Passive optical networks (PON) are one of the most widely growing access network technologies today [1, 2]. In PONs, an optical line terminal (OLT) delivers high data rates through an optical distribution network (ODN) to devices located in the user premises named optical network unit (ONU). A single OLT can serve between 16 to 128 ONUs at the same time using time division multiple access (TDMA). However, for future applications, TDMA alone is not sufficient. Wavelength division multiple access (WDMA) and optical code division multiple access (OCDMA) are two possible access schemes to be adopted in future access networks to increase both the data rate and the total number of subscribers served [3, 5].

OCDMA is a multi access technique that utilizes codes to distinguish between users that simultaneously access the optical media. Although OCDMA systems can potentially provide very high data rates, these systems suffer from multi access interference (MAI) [6]. MAI mitigation is a crucial part of any OCDMA detection design. Different OCDMA schemes have dealt with MAI mitigation in different ways ranging from simple passive approaches to highly complex coherent procedures [6]. A simple and low cost OCDMA scheme that cancels the MAI at the mean is known as spectral amplitude coding (SAC) OCDMA [7]. The main attributes of the SAC OCDMA is that the code signatures are encoded in spectral domain at the transmitter and the MAI is canceled at the receiver by a differential balanced detector.

Due to their spectral encoding, SAC OCDMA systems require broadband optical sources. Most of the literature have considered broadband incoherent sources such as light emitting diodes (LED) and amplified spontaneous emission (ASE) as SAC sources [8, 18]. Additional to their broadband nature, the low price of these sources makes them a natural choice if SAC OCDMA is ever going to be commercially viable as an access network technology. However, these sources suffer from intensity

*Corresponding author: ahmed7060@yahoo.com
Color versions of one or more of the figures in this paper are available online.

noise (IN) or phase induced intensity noise (PIIN) which limits their performance to support systems up to hundreds of Mb/s [19], not to mention the non uniform power distribution of the spectral bandwidth of these sources, which will lead to MAI if not processed by power equalization techniques [20, 21].

In order to overcome the above mentioned limitations of incoherent sources, the use of coherent sources in SAC OCDMA has been considered [22, 26]. It is important to note that coherent sources suffer from beat noise resulting from the laser signals overlapping in frequency [22]. This beat noise, if not mitigated, can result in limiting the performance of SAC OCDMA systems, even more than incoherent sources. Ayotte and Rusch [22] performed a capacity prediction comparing three different laser source configurations to incoherent sources alone and incoherent sources with forward error correction (FEC). They showed that for highly populated networks, a multi laser source with highly controlled lasers' central frequencies will provide the best performance. Yoshino et al. countered the beat noise by the use of coherent optical heterodyne detection [24]. The drawback of this scheme is that it requires high phase stabilization between the received signal and the local light signal. In [25] Yoshino et al. proposed a cost efficient well flattened multi wavelength source that can be used in SAC OCDMA as an alternative to the more expensive multi laser source. In [26], we proposed the use of wavelength multiplexed SAC OCDMA codes in order to improve the performance of highly populated coherent source SAC OCDMA networks.

In this paper we propose using spatial domain multiplexing to reduce the beat noise in the coherent source SAC OCDMA system. The use of spatial multiplexing is not new to SAC OCDMA. In [27] spatial multiplexing and 2D codes were used to reduce the PIIN in incoherent systems. By adopting spatial multiplexing we aim to divide the number of overlapping laser signals into two or more groups, where each group of signals is detected by a separate photodiode, leading to a reduction in the beat noise per spectral bin, and the system as a whole.

The rest of this paper is organized as follows; in Section II we show the structure of spatial multiplexing network and its transmitter and receiver. We evaluate our proposed system performance for the three different source configurations in Section III. In Section IV, we verify our proposed scheme through software simulation. Finally, a conclusion highlighting the major advantages and disadvantages of our proposed scheme is given in Section V.

II. SPATIAL MULTIPLEXING SAC OCDMA

Beat noise is generated at detection by two or more laser sources that have the same central frequency or a central frequency difference that falls within the receiver's bandwidth. The more the lasers satisfy the above condition, the higher the beat noise would be. The proposed scheme is based on dividing the number of overlapping laser signals into groups, where each group is detected separately by a different photodiode. By doing so, the total number of generated beat signals is reduced, and thus reducing the amount of distortion in the intended signal due to beat noise. For an N user network, we propose to split the number of users into two or more groups. Figure 1 shows a SAC OCDMA network that is divided into two groups. The first $N/2$ users are connected to star coupler *1* (SC_1) and the second $N/2$ users are connected to star coupler *2* (SC_2). For a maximum of L total laser signals per spectral bin, it is assumed that l_1 laser signals come from group 1 (via SC_1) and l_2 laser signals come from group 2 (via SC_2), where $L=l_1+l_2$. For example, for a SAC code that has a maximum of 12 overlapping lasers per spectral bin, if there are 7 laser signals coming from group *1* through SC_1, then there will be 5 laser signals coming from group *2* through SC_2. By applying this method, the total number of generated beat signals will be reduced.

The structure of the traditional SAC OCDMA transmitter

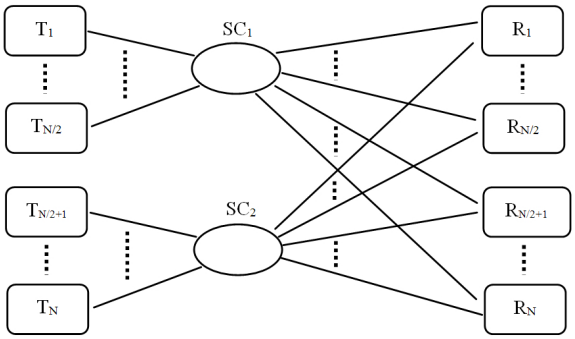

FIG. 1. Structure of the SM SAC OCDMA network. T: transmitter, SC: star coupler, R: receiver.

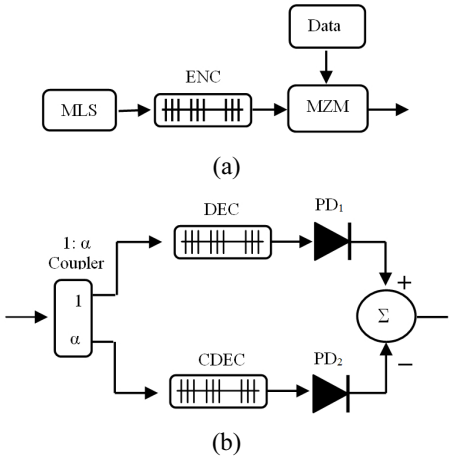

FIG. 2. Structure of the conventional SAC OCDMA. (a) transmitter, (b) receiver. MLS: multi laser source, MZM: Mach-Zehnder modulator, ENC: encoder, DEC: decoder, CDEC: complementary decoder, PD: photodiode.

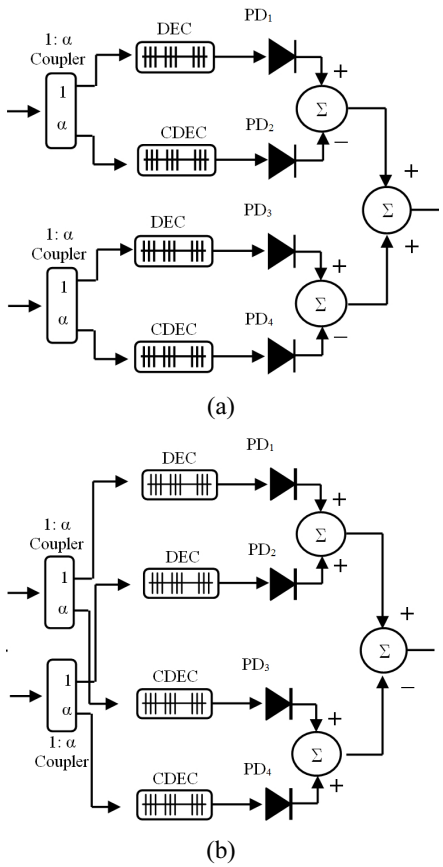

FIG. 3. Structure of the SM SAC OCDMA. (a) receiver, (b) alternative receiver design.

and receiver are given in Figs. 2(a) and (b), respectively. The receiver structure for our proposed scheme is given in Fig. 3(a). The structure of the SM SAC receiver is simply two balanced detectors connected in parallel. The output of SC_1 is connected to the first balanced detector and the output of SC_2 is connected to the second balanced detector for all receivers. At each balanced detector, the received signal is split into two by a coupler. The splitting ratio depends on the code family and the weight of the code in use. After splitting, the two signals are passed to either the decoder branch or the complementary decoder branch. The decoder branch is a group of filters that has a frequency response that passes the desired user's code signature. On the other hand, the complementary decoder is a group of filters whose frequency response is complementary to the decoder branch. The decoded signal (the desired user's signal and overlapping signals from other users) is passed to the upper photodiode of the balanced detector, and the complementary decoded signal is passed to the lower photodiode of the balanced detector. In order to cancel the MAI, the detected signal from the complementary decoder branch is subtracted from the detected signal from the decoder branch. The same procedure occurs at the second balanced detector for the other group of users. We would like to note that alternative receiver structure is given in Fig. 3(b) that has some minor changes.

The purpose of applying spatial multiplexing is to divide the number of overlapping laser signals per spectral bin into two or more groups, where each group is detected by a separate photodiode. Since the beat noise is the resultant of the square law of photo detection, the total number of generated beat signals will be reduced.

III. SYSTEM PERFORMANCE FOR THE SM SAC OCDMA

In this section, we predict the capacity of our proposed system. In our analysis we follow the same procedure used in [22].

3.1. Characteristic Functions Computation

In our performance analysis we try to find the expressions for the bit error rate (BER) when laser sources are used in SAC OCDMA. However, since there is no analytical expression for the intensity for more than two lasers that vary in phase and polarization, Monte Carlo simulation must be used [22]. The characteristic function of intensity for each spectral bin must be calculated. Using these characteristic functions, an expression for the probability density function can be derived and BER expressions can be found.

In our analysis we consider three different laser source configurations [22]. They are shared multi-laser source, uniformly distributed multi-laser source and controlled multi-laser source.

3.1.1. Shared multi laser source

In this case, there is a single centralized multi laser source shared by all users. The central frequencies for the different users for any spectral bin are perfectly aligned (because they come from the same source). However, the phase and polarization angles are random due to the different propagation distances from the centralized source to the users. The phase and polarization angles are assumed to be uniformly distributed in the range [0, 2π]. Fig. 4(a) shows the lasers alignment within a spectral bin in this configuration.

We conducted Monte Carlo simulation to obtain the probability density function (pdf) and the characteristics

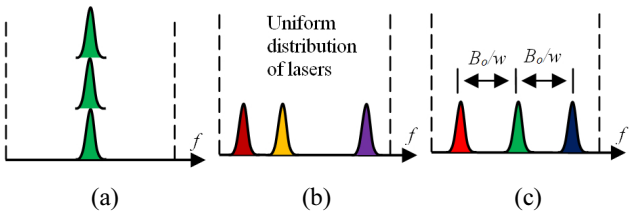

FIG. 4. Visual illustration of bin occupation by lasers for (a) shared multi laser source, (b) uniformly distributed multi laser source, (c) precisely controlled multi laser source [22].

function for user u averaged over different possibilities for phase and polarization angles.

The electrical field for a specific realization of phase and polarization i for user u is given by:

$$E_{u,i} = \begin{bmatrix} \sin(\beta_{u,i})\exp(\delta_{u,i}) \\ \cos(\beta_{u,i})\exp(\varphi_{u,i}) \end{bmatrix} \exp(j\omega_u t) \quad (1)$$

where $\beta_{u,i}$ is the angle of polarization, $\delta_{u,i}$ and $\varphi_{u,i}$ are the respective phases of the two polarization states. β, δ, and φ are random variables that are uniformly distributed over [0, 2π].

The intensity I generated from L user signals for a specific realization of phase and polarization is given by:

$$I_{L,i} = \left(\sum_{u=1}^{L} E_{u,i} \right) \left(\sum_{u=1}^{L} E_{u,i}^{*} \right) \quad (2)$$

We calculate the empirical distribution of the intensity for 10^7 different realizations for both phase and polarization. We assume that all the different realizations have the same probability i.e.$1/10^7$. The cumulative distribution function can be expressed as:

$$F(x|L) = \frac{1}{10^7} \sum_{i=1}^{10^7} 1_{\{I_{L,i} \le x\}} \quad (3)$$

where $1_{\{I_{L,i} \le x\}}$ is equal to "1" if x is greater than $I_{L,i}$ and "0" otherwise.

From the cumulative distribution function, (3), we can find the pdf:

$$f(x|L) = \frac{d(F(x|L))}{dx} \quad (4)$$

The characteristic function is the Fourier transform of the pdf in (4):

$$\Omega_I(\omega|L) = \int_{-\infty}^{\infty} f(x|L)\, e^{j\omega x} dx \quad (5)$$

When the number of laser sources is more than five, a good approximation of the characteristic function is obtained from the Gamma pdf instead of the empirical pdf [22].

3.1.2. Uniformly distributed multi laser source

Here, each user has its own multi-laser source. The central frequency of each laser for different users will fall within the bin bandwidth (B_o). However, due to manufacturing variations, the central frequencies will not be aligned but randomly distributed within the bin bandwidth. It is assumed the laser signals are uniformly distributed across the bin. Beating between laser sources can only occur if two or more laser signals fall at a distance no larger than the electrical bandwidth (B_e) away from each other. This can be interpreted mathematically by dividing B_o into r subdivisions, where each division is equal to B_e. Beat noise is generated if two or more lasers fall within the same subdivision. An illustration of the central frequency distribution within a spectral bin is given in Fig. 4(b).

The characteristic function for each spectral bin is given by [22]:

$$\Omega_I(\omega|L) = \sum_{\{m\}} \frac{|D_m|}{r^L} \Omega_I(\omega|L,m) \quad (6)$$

where m and D_m are the weight vector and occupancy vector, respectively.

3.1.3. Controlled multi laser source

In the third source configuration, not only are we assuming that each user has its own multi laser source, but that we can control the central frequencies of these laser signals to minimize the beat noise. For any given SAC code there is a maximum number of laser sources K that fall within any spectral bin. The spectral bandwidth B_o is divided into K equal spaced subdivisions and each laser source is assigned a subdivision. We assume that each laser's central frequency has a Gaussian distribution with a mean value being the central frequency of the allocated subdivision and the standard deviation is the level of precision of writing the laser's central frequency. The distribution of the laser's central frequencies within a bin for this case is given in Fig. 4(c).

The characteristics function in this case is given by [22]:

$$\Omega_I(\omega|L) = \sum_{B=0}^{L/2} P(B|L) \cdot \Omega_I(\omega|2)^B \cdot \Omega_I(\omega|1)^{L-2B} \quad (7)$$

where B is the number of laser pairs beating together, and $P(B|L)$ is the conditional probability for B pairs beating together out of L lasers.

3.2. BER Derivation

Assuming that there is a total number of L users, we start by dividing the number of users into two groups (more than two groups is possible, but we constrain our analysis to two groups). Users from 1 to $L/2$ are connected to the first coupler and users $L/2$ + 1 to L are connected to the second coupler. For each bin X in the decoder the number of lasers occupying spectral bin X reaching the decoder branch on the upper balanced detector (BD_1) and the lower balanced detector (BD_2) are b_{X_DEC1} and b_{X_DEC2}, respectively. Similarly, the number of lasers occupying spectral bin Y in the complementary decoder branch on the upper balanced detector and the lower balanced detector are b_{Y_CDEC1} and b_{Y_CDEC2}, respectively. The total number of

occupation for bin X in the decoder is given by:

$$b_{X\_DEC} = b_{X\_DEC1} + b_{X\_DEC2}$$

We assume that our desired user is first user and is located in the first group. We assume there are l interferers which are sending data "1", and these interferers are generated randomly, with the possibility of falling in the first group or the second group being equiprobable. We can say that:

$$l = l_1 + l_2$$

where l_1 and l_2 are the number of interferers coming from group one and group two, respectively.

For a specific pattern of l interferers, we compute the number of occupations for each bin in BD_1 and BD_2. Using the bin occupations we calculate the characteristic function derived in the previous section. The output of each balanced detector is computed by subtracting the detected intensity in the complementary decoder branch from the detected intensity of the decoder branch. The characteristic functions for each balanced detector is calculated by multiplying the characteristic functions of the contributing bins in the decoder with the characteristic functions of the contributing bins in the complementary decoder. We would like to note that the characteristic function is calculated as above due to the non overlapping nature of the different bins.

The characteristic functions when the desired user U is sending data "0", for BD_1 and BD_2 is given by:

$$\Omega_{BD1\_0}(\omega\,|U,T,l_1) = \left[\Omega_1(\omega\,|b_{1\_DEC1})\times\Omega_1(\omega\,|b_{X\_DEC1})\right] \times\left[\Omega_1(\omega/\alpha\,|b_{1\_CDEC1})\times\Omega_1(\omega/\alpha\,|b_{Y\_CDEC1})\right] \quad (8)$$

and

$$\Omega_{BD2\_0}(\omega\,|U,T,l_2) = \left[\Omega_1(\omega\,|b_{1\_DEC2})\times\Omega_1(\omega\,|b_{X\_DEC2})\right] \times\left[\Omega_1(\omega/\alpha\,|b_{1\_CDEC2})\times\Omega_1(\omega/\alpha\,|b_{Y\_CDEC2})\right] \quad (9)$$

and the characteristic functions for data "1" are:

$$\Omega_{BD1\_1}(\omega\,|U,T,l_1) = \left[\Omega_1(\omega\,|b_{1\_DEC1}+1)\times\Omega_1(\omega\,|b_{X\_DEC1}+1)\right] \times\left[\Omega_1(\omega/\alpha\,|b_{1\_CDEC1})\times\Omega_1(\omega/\alpha\,|b_{Y\_CDEC1})\right] \quad (10)$$

and

$$\Omega_{BD2\_1}(\omega\,|U,T,l_2) = \left[\Omega_1(\omega\,|b_{1\_DEC2})\times\Omega_1(\omega\,|b_{X\_DEC2})\right] \times\left[\Omega_1(\omega/\alpha\,|b_{1\_CDEC2})\times\Omega_1(\omega/\alpha\,|b_{Y\_CDEC2})\right] \quad (11)$$

where T is a binary data vector, whose elements represent the value of data each interferer is sending. The functions, Ω_{BD1_0}, Ω_{BD1_1}, Ω_{BD2_0}, and Ω_{BD2_1}, are the characteristic functions for the output of BD_1 and BD_2 when the desired user's data "0" and "1", respectively. b_{X_DEC1}, b_{Y_CDEC1}, b_{X_DEC2}, and b_{Y_CDEC2}, are the number of occupation for bin number X which is present in decoder branch and bin number Y which is present in the complementary decoder branch in BD_1 and BD_2. The variable a is the attenuation factor, and is present in the complementary decoder branch in order to cancel the MAI (this value depends on the code family and weight).

The previous calculation of characteristic functions is for a single combination of the data vector T. With different values of T, the number of occupation numbers b_{X_DEC1}, b_{X_DEC2}, b_{Y_CDEC1}, and b_{Y_CDEC2}, will vary. Assuming the values of vector T all have the same probability of occurrence, we average the characteristic functions for BD_1 and BD_2:

$$\Omega_{BD1\_0}(\omega\,|U,l_1) = E_T\left\{\Omega_{BD1\_0}(\omega\,|U,T,l_1)\right\} \quad (12)$$

and

$$\Omega_{BD2\_0}(\omega\,|U,l_2) = E_T\left\{\Omega_{BD2\_0}(\omega\,|U,T,l_2)\right\} \quad (13)$$

The same applies for Ω_{BD1_1}, Ω_{BD2_1}.

Assuming the number of users sending logical states "0" and "1" obey a binomial distribution, this yields a characteristic function for the desired user sending data "0" for the BD_1:

$$\Omega_{BD1\_0}\left(\omega\,|U,\frac{L}{2}-1\right) = \sum_{l_1=0}^{\frac{L}{2}-1}\left(\frac{1}{2}\right)^{\frac{L}{2}-1}\frac{\left(\frac{L}{2}-1\right)!}{l_1!\left(\frac{L}{2}-1-l_1\right)!}\Omega_{BD1\_0}(\omega\,|U,l_1) \quad (14)$$

and for BD_2:

$$\Omega_{BD2\_0}\left(\omega\,|U,\frac{L}{2}\right) = \sum_{l_2=0}^{\frac{L}{2}}\left(\frac{1}{2}\right)^{\frac{L}{2}}\frac{\left(\frac{L}{2}\right)!}{l_2!\left(\frac{L}{2}-l_2\right)!}\Omega_{BD2\_0}(\omega\,|U,l_2) \quad (15)$$

The same applies for Ω_{BD1_1}, Ω_{BD2_1}.

The electrical outputs of the two balanced detectors are added together to form the final decision statistics of the receiver, which is equivalent to the convolution of the pdfs. To generate the respective pdfs for each characteristic function, a Fourier transform is performed on each of the characteristic functions.

The pdf when the desired user is sending logical state "0":

$$f_0(x\,|U,L-1) = f_{BD1\_0}\left(x\,|U,\frac{L}{2}-1\right) * f_{BD2\_0}\left(x\,|U,\frac{L}{2}\right) \quad (16)$$

and for data "1":

$$f_1(x\,|U,L-1) = f_{BD1\_1}\left(x\,|U,\frac{L}{2}-1\right) * f_{BD2\_1}\left(x\,|U,\frac{L}{2}\right) \quad (17)$$

where f_{BD1_0}, f_{BD1_1}, f_{BD2_0}, and f_{BD2_1}, are the pdfs for BD_1 and BD_2 when the desired user is sending data "0" and "1".

Using a threshold value γ the BER is calculated from the pdfs by integrating the overlapping tales:

$$BER(U, L-1) = \frac{1}{2}\left(\int_{\gamma}^{\infty} f_0(x \mid U, L-1)dx + \int_{-\infty}^{\gamma} f_1(x \mid U, L-1)dx \right) \quad (18)$$

where γ is found numerically.

3.3. Results and Discussions

Firstly, to validate that spatial multiplexing can reduce the beat noise, an arbitrary bin Z that has 10 overlapping laser sources is considered. For the 10 overlapping laser sources (b=10), the pdf of intensity is computed with and without spatial multiplexing. Figure 5 shows the pdfs of intensity in both cases. The pdf without spatial multiplexing is generated for 10 laser sources using the method developed in Section III. In the case of spatial multiplexing, the 10 overlapping laser sources are divided between two photodiodes, where b_1 laser sources are present in the first photodiode and b_2 laser sources are present in the second photodiode. The pdf for b_1 (pdf_{b1}) and b_2 (pdf_{b2}) are generated. Since the contributing laser signals for b_1 and b_2 come from different sources and are received from different couplers and are detected by different photo detectors, it is safe to say that the signals from b_1 and b_2 are independent. Thus the accumulated pdf for bin Z (where $b=b_1+b_2$) is the convolution of pdf_{b1} and pdf_{b2}. As can be seen from Fig. 5 the pdfs with spatial multiplexing have smaller variance than the case without spatial multiplexing for all different values of b_1 and b_2. It can also be observed that the minimum variance is achieved when the number of laser signals falling within a bin is distributed equally between the two photodiodes. It is clear from the figures that spatial multiplexing leads to lower variance and thus lower beat noise.

In order to compare our results with published work, we choose the same operating parameters as in [22]. The data rates are 1.25 Gb/s, 2.5 Gb/s and 10 Gb/s and the optical bandwidth is 30 nm. Two balanced incomplete block design (BIBD) codes are implemented. The first is a code with prime power of 5 (q=5) and cardinality of 31, and the second is a code with q=11 and cardinality of 133. The bin spectral width is 0.97 nm and 0.23 nm for code one and code two, respectively.

Figures 6(a) and (b) show the BER versus the number of users at 1.25 Gb/s for the lower and higher cardinality codes, respectively. It can be clearly seen from Fig. 6(a) that the SM SAC outperforms the conventional SAC for all different coherent source configurations. From Fig. 6(a), as an example of the performance improvement, the SM SAC with controlled multi laser source with a standard deviation of 4 GHz for precision of writing the central frequency can support around 25 active users at BER of 10^{-9} (error free transmission), meanwhile for the same source configuration at the same BER the conventional SAC can

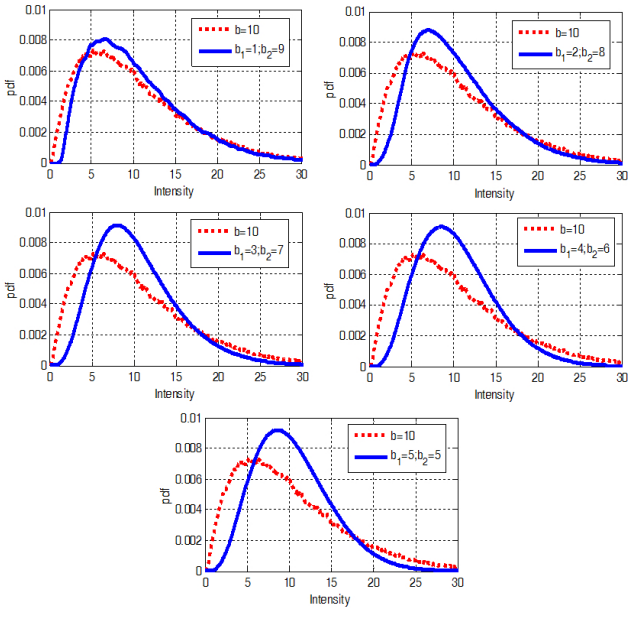

FIG. 5. The pdf of intensity for 10 overlapping lasers for SAC OCDMA bin and SM SAC OCDMA bin with different bin occupations.

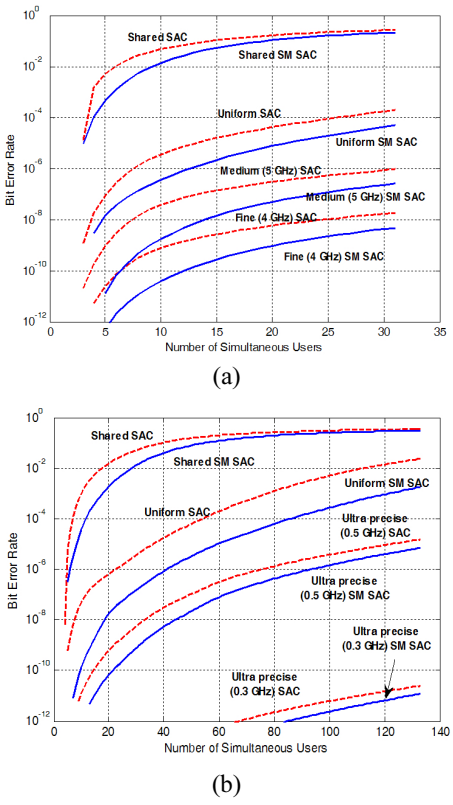

FIG. 6. BER versus the active number of users at 1.25 Gb/s and an optical bandwidth of 30 nm for (a) BIBD code (q=5), (b) BIBD code (q=11).

only support 10 users. For a precision of 3 Ghz (not shown in the Fig. 6(a)) both SAC and SM SAC supported all the users for a BER of 10^{-10}, with SM SAC showing better performance than the conventional SAC. Fig. 6(b) shows that the SM SAC will also have higher performance than the conventional SAC for a code with larger weight and higher cardinality. For the uniform multi laser source, the SAC can only support 5 users at BER of 10^{-9}, while the SM SAC can support 15 users. In the case of the precisely controlled multi laser, we can see for a standard deviation of 0.3 nm of the central frequency the SM SAC

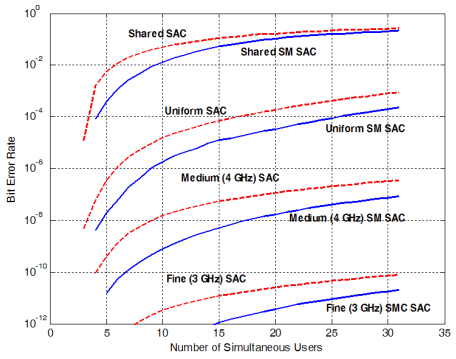

(a)

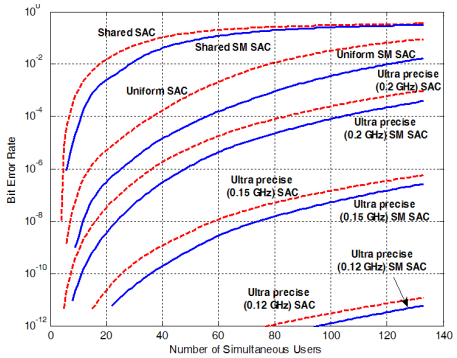

(b)

FIG. 7. BER versus the active number of users at 2.5 Gb/s and an optical bandwidth of 30 nm for (a) BIBD code (q=5), (b) BIBD code (q=11).

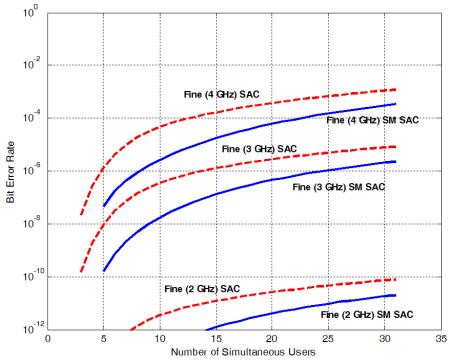

FIG. 8. BER versus the active number of users at 10 Gb/s and an optical bandwidth of 30 nm for a BIBD code (q=5).

can maintain up to 85 active users at BER of 10^{-12}, in the meantime, the conventional SAC can bear just above 65 users at the same BER, a 30% increase.

Figures 7(a) and (b) show the BER versus the active number of users for the same two codes at 2.5 Gb/s, meanwhile Fig. 8 shows the BER versus the number active users for code (q=5) for data rate of 10 Gb/s. The first observation from these figures is that there is performance degradation for both conventional SAC and SM SAC compared to 1.25 Gb/s data rate figures due to the larger electrical bandwidth. Secondly, for the precisely controlled multi laser source configuration, a tighter precision is required for the central frequency to achieve similar performance, which is also due to the higher data rate. By looking at Figures 7(a) and (b) we see that for a higher data rate the SM SAC outperforms the conventional SAC for both codes. As an example of the performance superiority, for a tightly controlled central frequency (standard deviation of 0.12 nm) multi laser source, the SM SAC was able to achieve around 95 simultaneous users, while the conventional SAC was able to bear just below 80 users. From Fig. 8 we can see that for 10 Gb/s much higher precision in the central frequency is required to achieve a similar BER as the previous data rates. To achieve a BER of 10^{-10} or less for all number of users a central frequency precision of 2 GHz is required for both conventional SAC and SM SAC. It is clear from the figure that the SM SAC shows some significant performance improvement over the conventional SAC.

We would like to note that the percentage of improvement obtained by the SM SAC over the conventional SAC depends on the source configuration and the data rate.

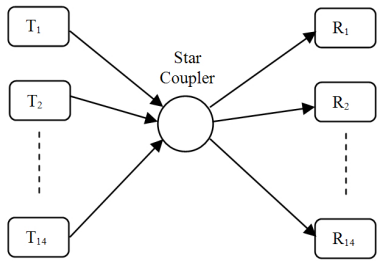

(a)

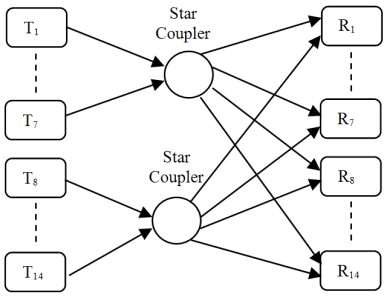

(b)

FIG. 9. Network configuration for both (a) SAC, (b) SM SAC. T: transmitter, SC: star coupler R: receiver.

IV. SOFTWARE SIMULATION

4.1. Simulation Setup

The software we used for our simulation is Optisystem. For the simulation we chose the third source configuration, i.e. the precisely controlled multi laser source. We implemented a fourteen user network for both the conventional SAC and SM SAC (two groups), and the network configurations are shown in Figs. 9(a) and (b), respectively. The code used is BIBD code with prime power of 2 (weight=3) multiplexed in the wavelength domain using the technique given in [26, 28]. Table 1 shows the code sequence for the fourteen users.

In our design, each transmitter contains a controlled multi laser source. By carefully observing Table 1, we can see that the maximum number of laser sources falling in one spectral bin is three. Since we can control the lasers' central frequencies, we assigned one of the lasers' central frequencies to the central frequency of the spectral bin. The other two lasers are placed at 0.2 nm to the right and left of the centralized bin. A visual illustration of the lasers distribution within a given spectral bin is shown in Fig. 10.

The transmitter for both conventional SAC and SM SAC contains three controlled lasers. The default launch power for each laser is 0 dBm. The signals from the lasers are summed up and modulated with the data of a pseudo random bit sequence (PRBS) generator via Mach-Zehnder modulator (MZM) which has an extinction ratio of 30 dB. After modulation, the signals are sent to the network as shown in Figs. 9(a) and (b).

The receiver designs are similar to the designs given in Fig. 2(b) and Fig. 3(a). Fiber Bragg gratings (FBG) filters in reflection are used in the decoder and complementary decoder designs. All the FBGs have 0.6 nm pass bandwidth. The photodiodes for both the conventional SAC and SM SAC receivers are the standard PIN photodiodes. The receiver's electrical filter is a fourth order Bessel filter with an electrical bandwidth equal to 0.75×data rate.

4.2. Results

Figure 11 shows the results for the BER as the number of users is increased from two to fourteen at a data rate of 1.25 Gb/s. It can be seen that both the conventional SAC

TABLE 1. BIBD wavelength multiplexed code with weight of three

User #	Code Sequence													
User #1	0	0	0	1	0	1	1	0	0	0	0	0	0	0
User #2	0	0	1	0	1	1	0	0	0	0	0	0	0	0
User #3	0	1	0	1	1	0	0	0	0	0	0	0	0	0
User #4	1	0	1	1	0	0	0	0	0	0	0	0	0	0
User #5	0	1	1	0	0	0	1	0	0	0	0	0	0	0
User #6	1	1	0	0	0	1	0	0	0	0	0	0	0	0
User #7	1	0	0	0	1	0	1	0	0	0	0	0	0	0
User #8	0	0	0	0	0	0	0	0	0	0	1	0	1	1
User #9	0	0	0	0	0	0	0	0	0	1	0	1	1	0
User #10	0	0	0	0	0	0	0	0	1	0	1	1	0	0
User #11	0	0	0	0	0	0	0	1	0	1	1	0	0	0
User #12	0	0	0	0	0	0	0	0	1	1	0	0	0	1
User #13	0	0	0	0	0	0	0	1	1	0	0	0	1	0
User #14	0	0	0	0	0	0	0	1	0	0	0	1	0	1

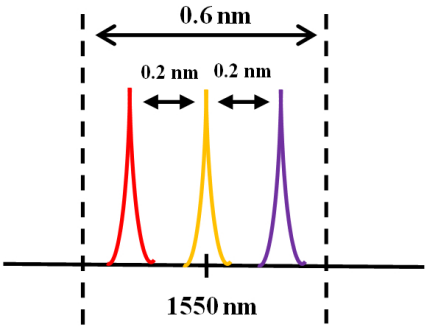

FIG. 10. Laser central frequency assignments within a given spectral bin.

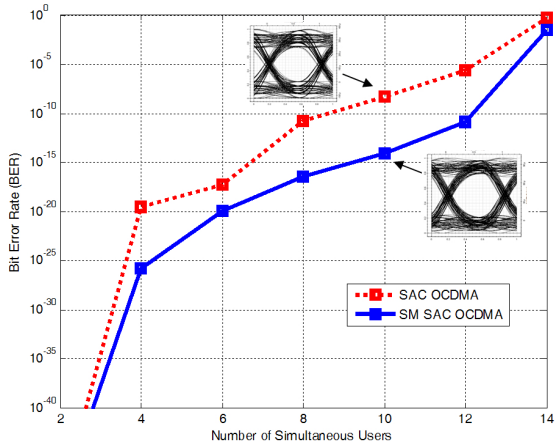

FIG. 11. BER versus number of active users at 1.25 Gb/s.

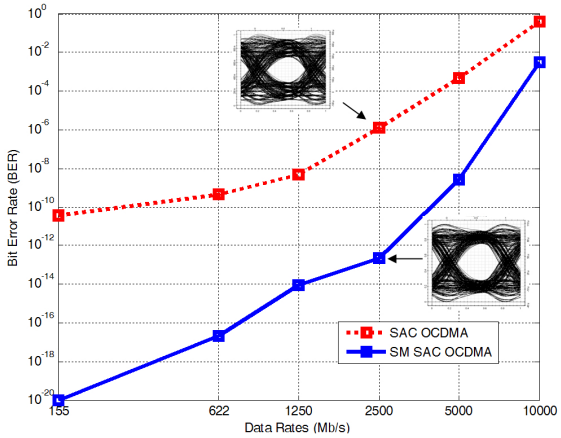

FIG. 12. BER versus different data rates for ten active users.

and SM SAC are able to achieve error free transmission, with some BER improvement on SM SAC compared to conventional SAC for up to eight active users. However, when ten users are active, the conventional SAC transmission is erroneous, with a reported BER of 4.95×10^{-9}. Meanwhile, SM SAC sustained error free transmission for up to twelve users, and the reported BER was 1.2×10^{-11}. The eye diagrams for both cases for ten active users are illustrated in Fig. 11, which clearly show the improved quality of the received signal for SM SAC compared to conventional SAC. For a fully populated network (fourteen users in our simulation), both conventional SAC and SM SAC failed to achieve error free transmission. The reported BER for fourteen users for both conventional SAC and SM SAC were 0.6 and 3.49×10^{-2}, respectively. We would like to note that the very low BER (below 10^{-20}) is due to the small number of users (2 to 6 users) where the beat noise is negligible.

The BER at different data rates for ten active users is shown in Fig. 12. SM SAC was able to achieve error free transmission up to 2.5 Gb/s, with a reported BER value of 2.3×10^{-13} at 2.5 Gb/s. On the other hand, conventional SAC was able to achieve error free transmission at only 155 Mb/s and 622 Mb/s data rates. The eye diagrams at 2.5 Gb/s are given in the figure to qualitatively show the difference in the received signals in both cases. For 10 Gb/s transmission both conventional SAC and SM SAC were unable to retrieve the transmitted data.

By observing Figs. 11 and 12, we can conclude that the obtained results agree with the results obtained via Monte Carlo simulation, and some form of confirmation can be drawn that SM SAC will always outperform conventional SAC at any number of users and at any data rate. To support more active users and to achieve error free transmission at higher data rates, a code with a higher weight (and naturally a larger optical bandwidth) can be used, or by the use of wavelength multiplexed codes.

V. CONCLUSION

In conclusion, in this paper we adopted a spatial multiplexing scheme to mitigate the beat noise in coherent source SAC OCDMA network. By applying spatial multiplexing we were able to reduce the beat noise via reducing the total number of generated beat signals per spectral bin. In our analysis we considered three different coherent source configurations. Our results from Monte Carlo simulation showed our proposed scheme outperformed the conventional SAC for all the three different source configurations. A 30% increase in the number of users was reported for a precisely controlled multi laser source at 1.25 Gb/s and reference BER of 10^{-12}. To back up our results from the Monte Carlo simulation we performed an optical software simulation for fourteen active users for the precisely controlled multi laser source configuration. Results showed that SM SAC was able to achieve error free transmission up to twelve users at a data rate of 1.25 Gb/s. Meanwhile, the conventional SAC scheme could only support eight users at the same data rate. Furthermore, for ten active users the SM SAC was able to maintain error free transmission up to 2.5 Gb/s, while the conventional SAC could only support up to 622 Mb/s.

In order to enable a more active number of users at higher data rates the code space should be divided into more than two groups. However, this will require more optical fibers and photonics devices.

REFERENCES

1. I.-T. R. G. 987.1:, 10-Gigabit-Capable Passive Optical Networks (XG-PON): General Requirements (2010).
2. IEEE P802.3av Task Force, "10Gb/s ethernet passive optical network," http://www.ieee802.org/3/av/.
3. B.-W. Kang and C.-H. Kim, "An amplified WDM-PON using broadband light source seeded optical sources and a novel bidirectional reach extender," J. Opt. Soc. Korea **15**, 222-226 (2011).
4. S.-H. Yoo, S.-G. Mun, J.-Y. Kim, and C.-H. Lee, "1.25 Gb/s broadcast signal transmission in WDM-PON based on mutually injected Fabry-Perot laser diodes," J. Opt. Soc. Korea **16**, 101-106 (2012).
5. Z. A. El-Sahn, B. J. Shastri, M. Z. M. Zeng, N. Kheder, D. V Plant, and L. A. Rusch, "Experimental demonstration of a SAC-OCDMA PON with burst-mode reception: local versus centralized sources," J. Lightwave Technol. **26**, 1192-1203 (2008).
6. H. Ghafouri-Shiraz and M. Karbassian, *Optical CDMA Networks: Principles, Analysis and Applications* (Wiley, 2012).
7. D. Zaccarin, S. Member, and M. Kavehrad, "An optical CDMA system based on spectral encoding of LED," IEEE Photon. Technol. Lett. **4**, 479-482 (1993).
8. M. Abtahi, S. Ayotte, S. Member, J. Penon, L. A. Rusch, and S. Member, "Balanced detection of correlated incoherent signals: a statistical analysis of intensity noise with experimental validation," J. Lightwave Technol. **26**, 1330-1338 (2008).
9. J. Penon, W. Mathlouthi, S. LaRochelle, and L. A. Rusch, "An innovative receiver for incoherent SAC-OCDMA enabling SOA-based noise cleaning: experimental validation," J. Lightwave Technol. **27**, 108-116 (2009).
10. A. Ghazisaeidi and L. A. Rusch, "Capacity of SOA-assisted SAC-OCDMA," IEEE Photon. Technol. Lett. **22**, 441-443 (2010).
11. C. Yang, "Spectral amplitude coding optical CDMA networks using 2^m×2^m waveguide gratings," IEEE Photon. Technol. Lett. **22**, 1835-1837 (2010).
12. M. Noshad and K. Jamshidi, "Code family for modified spectral-amplitude-coding systems and performance analysis," OSA J. Opt. Netw. **2**, 344-354 (2010).
13. A. M. Alhassan, N. M. Saad, and N. Badruddin, "An enhanced detection technique for spectral amplitude coding optical CDMA systems," IEEE Photon. Technol. Lett. **23**, 875-877 (2011).
14. M. Noshad and K. Jamshidi, "Bounds for the BER of

codes with fixed cross correlation in SAC-OCDMA systems," J. Lightwave Technol. **29**, 1944-1950 (2011).
15. H. Chen, S. Xiao, L. Yi, Z. Zhou, M. Zhu, J. Shi, Y. Dong, and W. Hu, "A tunable encoder/decoder based on polarization modulation for the SAC-OCDMA PON," IEEE Photon. Technol. Lett. **23**, 748-750 (2011).
16. H. M. H. Shalaby, "Closed-form expression for the bit-error rate of spectral-amplitude-coding optical CDMA systems," IEEE Photon. Technol. Lett. **24**, 1285-1287 (2012).
17. H. M. H. Shalaby, "Efficient use of PPM in spectral-amplitude-coding optical CDMA systems," J. Lightwave Technol. **30**, 3512-3519 (2012).
18. H. M. R. Al-Khafaji, S. A. Aljunid, A. Amphawan, H. A. Fadhil, and A. M. Safar, "Reducing BER of spectral-amplitude coding optical code-division multiple-access systems by single photodiode detection technique," J. Eur. Opt. Soc. Rapid Publ. **13022**, 1-5 (2013).
19. E. D. J. Smith, R. J. Blaikie, and D. P. Taylor, "Performance enhancement of spectral-amplitude-coding optical CDMA using pulse-position modulation," IEEE Trans. Commun. **46**, 1176-1185 (1998).
20. J.-F. Huang, C.-M. Tsai, and Y.-L. Lo, "Compensating fiber gratings for source flatness to reduce multiple-access interferences in optical CDMA network coder/decoders," J. Lightwave Technol. **22**, 739-745 (2004).
21. S. S. Pawar, R. K. Shevgaonkar, and A. Karandikar, "Improved SAC-OCDMA system with multiple incoherent sources," IEEE Photon. Technol. Lett. **20**, 2099-2101 (2008).
22. S. Ayotte and L. A. Rusch, "Increasing the capacity of SAC-OCDMA: forward error correction or coherent sources?," IEEE J. Select. Topic Quantum Electron. **13**, 1422-1428 (2007).
23. A. T. Pham, N. Miki, and H. Yashima, "Spectral-amplitude-encoding optical-code-division-multiplexing system with a heterodyne detection receiver for broadband optical multiple-access networks," OSA J. Opt. Netw. **4**, 621-631 (2005).
24. M. Yoshino, S. Kaneko, T. Taniguchi, N. Miki, K. Kumozaki, T. Imai, N. Yoshimoto, and M. Tsubokawa, "Beat noise mitigation of spectral amplitude coding OCDMA using heterodyne detection," J. Lightwave Technol. **26**, 962-970 (2008).
25. M. Yoshino, N. Miki, N. Yoshimoto, and K. Kumozaki, "Multiwavelength optical source for OCDM using sinusoidally modulated laser diode," J. Lightwave Technol. **27**, 4524-4529 (2009).
26. A. M. Alhassan, N. Badruddin, N. M. Saad, and S. A. Aljunid, "Performance analysis of wavelength multiplexed SAC OCDMA codes in beat noise mitigation in SAC OCDMA systems," J. Eur. Opt. Soc. Rapid Publ. **8**, 1-9 (2013).
27. C.-C. Yang and J.-F. Huang, "Two-dimensional M-matrices coding in spatial/frequency optical CDMA networks," IEEE Photon. Technol. Lett. **15**, 168-170 (2003).
28. C.-C. Yang, "Hybrid wavelength-division-multiplexing/spectral-amplitude-coding optical CDMA system," IEEE Photon. Technol. Lett. **17**, 1343-1345 (2005).